Digest Journal of Nanomaterials and Biostructures Vol. 8, No. 4, October – December 2013, p. 1491 - 1507

DIMENSIONAL EFFECT OF MICROCHANNELS ON MICROFLUIDIC ELECTROKINETIC INSTABILITY

KAO-FENG YARN[a], I-TING HSIEH[b], YU-JEN PAN[c], WEN-CHUNG CHANG[b], WIN- JET LUO[d*]
[a]*Department of Electronic Engineering, Far East University, Hsin-Shih, Tainan, Taiwan*
[b]*Department of Electronic Engineering, Southern Taiwan University of Technology, Taiwan*
[c]*Department of Digital Content and Technology, Ta Hwa University of Science and Technology, Hsinchu 307, Taiwan*
[d]*Graduate Institute of Precision Manufacturing, National Chin-Yi University of Technology, Taichung, Taiwan*

Electrokinetic force occurs when fluid flows with an electric conductivity gradient are driven by external electric field. It is proportionally related to the electric field intensity. When the applied electric field intensity is below certain critical value, the effect of electrokinetic force on the fluid flows is smaller, and the flows are as stable as electroosmotic flow. While the applied electric field intensity exceeds certain critical value, greater electrokinetic force occurs on the flows, and the flows may induce unstable perturbation in the interface. This perturbation can be used to accelerate microfluidic mixing. However, joule heating problems often occur due to high intensity of critical electric field when electrokinetic force is used to achieve microfluidic mixing. In this study, we found microchannel width may affect electric conductivity gradient between fluids, and further critical electric field intensity. By means of experience and theoretical simulation, it has been found that electrokinetic instability phenomenon may easily occur in narrower microchannels while the phenomenon in the wider microchannels requires higher electric field intensity. This study designed sharply reduced microchannels to promote electrokinetic instability and reduce required critical electric field intensity.

(Received July 11, 2013; Accepted October 30, 2013)

Keywords: Electroosmotic flow, Electrokinetic instability, Microfluidics.

1. Introduction

Over the past twenty years, many integrated electrokinetic microsystems have been developed with a wide range of functionalities, including sample pretreatment, mixing, separation, and so forth. Such systems are a key component of so-called micro-total-analysis systems, which aim to integrate multiple chemical analysis functions on a single microfabricated chip. After miniaturization, the traditional medical instruments are based on the microchips which can reduce operation procedure, operation error, consumption of great reagent and operation costs, and quickly and concurrently deal with mass biological information. In combination with biomedicine and MEMS process system, the instruments are called Bio-MEMS [1-3]. In testing, samples and regents usually need to be fully mixed in the microchips. However, due to lower Reynolds numbers of the flows in the microchips, the flows in the microchannels are laminar flows. In case of no turbulent flow, it is rather difficult to mix fluids in a limited length and time. In order to mix

* Corresponding author: wjluo@ncut.edu.tw

the fluids quickly, the device of microfluidic mixer was developed to efficiently mix the sample and reagent within the microchannels. Micro-mixers can be divided into active and passive types. Microchannels of the passive mixers are complicated in structure and the corresponding mixing efficiencies are not apparent. The active mixers need additional devices to enhance the mixing process, which are not easy to integrate with the chips.

However, as the complexity of these systems increase, achieving a robust control of electrokinetic processes involving heterogeneous samples becomes increasingly important. A common concern in the microfluidics field is that of on-chip biochemical assays with high conductivity gradients. These gradients may occur intentionally, as is the case in sample stacking processes, or unintentionally, as in the case of multi-dimensional assays. Such conductivity gradients are known to result in flow instability when the fluids are driven by an external electrical field of high intensity. The presence of these electrokinetic instabilities, commonly referred to as EKI, can be regarded as a particular form of electrohydrodynamic instability, which is generally associated with electroosmotic flow. For the literatures about EKI, Melcher and Taylor [4] and Saville [5] developed Ohmic models to describe the instability of electrohydrodynamic flows under the assumption of zero interfacial electrokinetic effects. Hoburg and Melcher [6] performed a stability analysis of microfluidic flow in which the external electrical field was applied parallel to the liquid–liquid interface. Baygents and Baldessari [7] performed an analysis of electroosmotic flow taking the effect of the effects of conductivity diffusion into account and showed that flow become unstable when the intensity of the applied electric field exceeded a certain value. Lin et al. [8] used a long rectangular cross-section in which the conductivity gradient was orthogonal to the main flow direction. The results showed flow system became highly unstable when the electrical field intensity exceeded a critical threshold value. Oddy and Santiago [9] presented a four-species electrokinetic instability model to investigate electroosmotic flow in a high aspect ratio geometry with a base state in which the conductivity gradient was orthogonal to the applied electrical field. The numerical simulation results were shown to be in good qualitative agreement with the experimental image data for electrolyte solutions with a conductivity ratio of 1.05:1. In the literature, Posner and Santiago [10] introduced two liquids with different conductivity and concentration into the cross-type channel, and induced EKI with DC electric field. Chen et al. [11] studied the EKI phenomenon in a T-type microchannel. The authors performed a linear stability analysis on an electrokinetic instability model and applied Briggs-Bers criteria to identify physically unstable modes and to determine the nature of the instability.

In addition, many scholars discussed feasibility of using EKI phenomenon in microfluidic mixing. Shin et al. [12] introduced liquids with different conductivity into cross-type channel by applying DC electric field to observe the perturbation frequency of EKI, and then applied AC electric field to main channel. In the study, the optimal mixing efficiency can be achieved when frequency of AC electric field is equal to half of the perturbation frequency in the DC electric field. Park et al. [13] designed main channel of the T-type channels to be symmetrical Y shaped, and introduced the liquids with different conductivity and concentration. After applying DC electric field, vortex occurred in sharp corner of the main channel. The vortex increased mixing efficiency. Oddy et al. [14] introduced two liquids with different electric conductivity into T-type channels by imposing pressure, plated channels with electrodes, and induced EKI phenomenon to increase mixing efficiency by applying electric field to the electrodes. Tai et al. [15] and Pan et al. [16] suggested valveless switching and EKI mechanism to transmit mixing liquid to specific outlet and increase mixing efficiency. Luo et al. [17-20] used electric field perturbation to enhance EKI and increase mixing effect in the T-type microchannels. Besides, Cho et al. [21] suggested simulation of cross-type microfluid mixers based on a periodic time-varying EKI. This system produces a periodic oscillation to adjust potential perturbation in channels. From the simulation, it can be found mixing efficiency can be increased through proper geometric shape and perturbation parameters.

From the previous literature, when the applied electric field is higher than certain critical value, the electrokinetic force may cause the fluid flows to generate perturbation in the interfaces of the fluid. Although the effects enhance solution mixing, the relatively high value of the electric

field intensity at which EKI is induced limits the practicability of microfluidic mixing applications. Thus, finding a way to reduce high intensity of electric field at which EKI is induced, and maintaining high mixing efficiency will become a research subject. In this study, concave and convex geometrical shapes were etched first in the microchannels to increase electric conductivity gradients on the fluid path, and further produce microfluidic components which can improve electric field critical value and enhance mixing efficiency.

2. Method

2.1 Fabrication

The current microchannels were fabricated using glass substrates (Ø100mm/1mm, Fair & Cheer Inc., Taiwan). The details of the fabrication process are presented in the literature [22] and are therefore discussed briefly in the following. Fig. 1 Illustrates the simplified fabrication process for devices are based on glass substrates. Initially, a thin layer of AZ4620 positive photoresist was firstly spin-coated on the glass slide for the pattern definition and was use as the etching mask for glass etching. The patterned substrate was then immersed into BOE solution to generate 20-μm deep microchannels. Note that the substrate was immersed into a 1 M HCl solution for 10 s every 5 min during the etching process for removing the precipitations. The photoresist layer was then removed using an acetone solution. Fluid via-holes were drilled using a diamond drill bit on another bare upper substrate. The microchip was then sealed in a sintering oven at 580°C for 10 min.

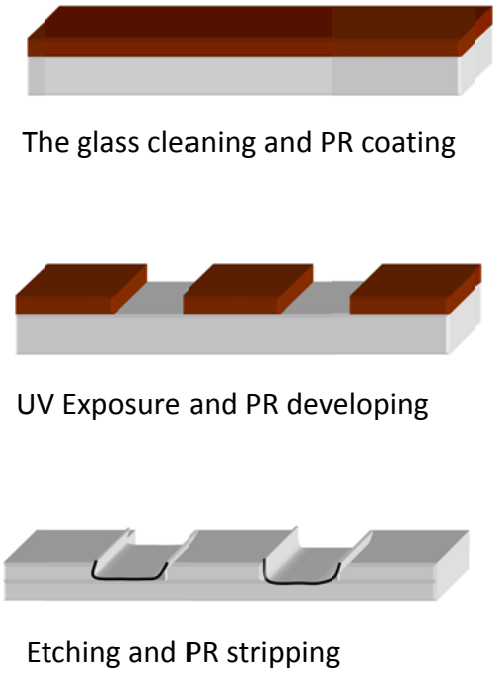

Fig. 1. Simplified fabrication process for devices are based on glass substrates.

2.2 Experimental setup

The fluid sample manipulations within the microchip are observed by a mercury lamp induced fluorescence technique using a charge-coupled device camera (CCD, model SSC-DC50A, Sony, Japan). The electrokinetic driving forces are generated by means of a high voltage power supply (model MP-3500, Major Science, Taiwan) operating under the control of a PC. The experimental images are captured by an optical microscope (model Eclipse 50I, Nikon, Japan), filtered spectrally, and then measured by the CCD device.

2.3 Formula

The glass microchannel considered in the present study has height of 60 μm. The channel is filled with a monovalent binary electrolyte of uniform viscosity, μ and permittivity, ε. Since the characteristic height of the glass microchannel is in the order of magnitude of 10 mm, the interaction between the fluid and the wall is significant and must therefore be explicitly considered in the theoretical model. A review of the related literature suggests that an Ohmic model [4] for electrolytic solutions, and the Navier-Stokes equation with electric body force term provides a reasonable description of the electrokinetic instability flow in the present glass microchannel. In this model, the distributions of the electrical conductivity (σ) and the electrical field (φ), respectively, are both described by the electrolytic Ohmic model by assuming electroneutrality and negligible diffusive current. For a monovalent binary electrolyte which is fully dissociated, charge density (ρ_f) and electric conductivity are related to concentration of cations (c_+) and anions (c_-) through

$$\rho_f = F\left(c_+ - c_-\right)$$

$$\sigma = F^2\left(c_+ b_+ + c_- b_-\right)$$

Where F is the Faraday constant, m is ionic mobility. Under electro-neutrality, $c_+ = c_- = c$, where c is the reduced ionic concentration, and the conductivity is proportional to this reduced ionic concentration by $\sigma = F^2\left(b_+ + b_-\right)c$. The conservation equations of charged species can be combined to yield,

$$\frac{\partial c}{\partial t} + \left(\vec{V}\cdot\nabla\right)c = D_{eff}\nabla^2 c, \tag{1}$$

$$\nabla\cdot\vec{i} = 0, \tag{2}$$

where $\vec{V}$ is fluid velocity and $\vec{i}$ is current density. The effective diffusivity D_{eff} is defined as:

$$D_{eff} = \frac{2D_+ D_-}{D_+ + D_-}$$

where $D_\pm$ is ionic diffusivity, and is related to mobility by Einstein's relation $D_\pm = R\,T\,b_\pm$ where R is the universal gas constant, and T is temperature. By assuming negligible diffusive current, the current density can be yield to $\vec{i} \cong \sigma\,\vec{E}$ where $\vec{E}$ is electric field intensity. Appling the linear relationship between reduced concentration and conductivity, Eq. (1) and (2) reduce to

$$\frac{\partial\sigma}{\partial t} + \left(\vec{V}\cdot\nabla\right)\sigma = D_{eff}\nabla^2\sigma, \tag{3}$$

$$\nabla\cdot\left(\sigma\,\vec{E}\right) = 0. \tag{4}$$

The electric field intensity is related to electric potential ϕ by $\vec{E} = -\nabla\phi$. The conductivity distribution and electric field are governed by the electrolytic Ohmic model, Eqs (3) and (4), and the electroosmotic flow is described by the incompressible Navier-Stokes equation, i.e.

$$\frac{\partial\sigma}{\partial t} + \left(\vec{V}\cdot\nabla\right)\sigma = D_{eff}\nabla^2\sigma, \tag{5}$$

$$\nabla \cdot \left(\sigma \nabla \phi \right) = 0, \tag{6}$$

$$\nabla \cdot \vec{V} = 0, \tag{7}$$

$$\rho \frac{\partial \vec{V}}{\partial t} + \rho \left(\vec{V} \cdot \nabla \right) \vec{V} = -\nabla p + \mu \nabla^2 \vec{V} + \varepsilon \left(\nabla^2 \phi \right) \nabla \phi, \tag{8}$$

where ρ is the mass density, p is the pressure and μ is the dynamic viscosity of the working fluid. Under electroneutrality, the electrical conductivity can be viewed as a material property which obeys a convective diffusion equation, Eq. (5). Equation (6) is simply Kirchhoff's Law valid for the special case where Ohmic current dominates. Through the electric body force in the momentum equation, Eq. (8), the electric field is coupled to the electroosmotic flow. In this model, electrical conductivity is not a passive scalar because a change in conductivity will alter the electric field and induce net charge, and the resulting electric body force will alter the velocity field.

In the current simulations, it is assumed that the physics of the electrical double layer (EDL) influence the instability dynamics only in that the EDL determines the electroosmotic velocity in the immediate vicinity of the glass microchannel wall. This assumption is supported by the fact that the EDLs adjacent to the current glass microchannel walls have a characteristic Debye length (λ_D) of less than 10 nm, which is considerably less than the characteristic channel width and height. The zeta potential on the homogeneous surface of the glass microchannel is assigned a value of -75 mV in this study. Thus, the boundary conditions at the walls, inlets, and outlet of the glass microchannel are given, respectively, by:

1. At the walls, with non-penetrable condition:

$$n \cdot \nabla \sigma = 0,$$
$$n \cdot \nabla \phi = 0,$$

For horizontal wall, with slip conditions:

$$u = -\frac{\varepsilon \zeta}{\mu} \frac{\partial \phi}{\partial x}, \quad v = 0$$

$$\frac{\partial P}{\partial x} = \mu \frac{\partial^2 u}{\partial x^2} + \varepsilon \left(\frac{\partial^2 \phi}{\partial x^2} + \frac{\partial^2 \phi}{\partial y^2} \right) \frac{\partial \phi}{\partial x}$$

For vertical wall, with slip conditions:

$$u = 0, \quad v = -\frac{\varepsilon \zeta}{\mu} \frac{\partial \phi}{\partial y}$$

$$\frac{\partial P}{\partial y} = \mu \frac{\partial^2 v}{\partial y^2} + \varepsilon \left(\frac{\partial^2 \phi}{\partial x^2} + \frac{\partial^2 \phi}{\partial y^2} \right) \frac{\partial \phi}{\partial y},$$

where n denotes the wall-normal direction and ζ is the zeta potential of the EDL. The boundary conditions are consequences of the non-penetrable nature of the glass microchannel walls. (u, v) are the flow velocity in the X- direction and Y- direction respectively. The electroosmotic velocity at the wall is a function of the local ionic concentration and the electrical field strength, and is given by the Smoluchowski equation. The value of the zeta potential is related to the ionic concentration, which is proportional to the ionic conductivity for dilute solutions under electro-neutrality conditions. In modeling the zeta potential, the following correlation is assumed: $\varsigma / \varsigma_r = \left(\sigma / \sigma_r \right)^{-k}$, where k is an empirical constant and ζ_r is the reference zeta potential at the

reference conductivity of σ_r . Note that in this study, *k* and reference zeta potential are assigned of zero and -75mv, respectively. Thus, zeta potential, ζ , on the homogeneous surface of the glass microchannel is -75mv.

2. At the inlets:

$$\sigma = C_{EP}$$

$$\frac{\partial u}{\partial y} = 0, \quad \frac{\partial v}{\partial y} = 0, \quad P = 0, \quad \frac{\partial \sigma}{\partial y} = 0,$$

where C_{EP} is the value of constant electric potentials applied at the inlets.

3. At the outlet:

$$\phi = 0, \quad \frac{\partial u}{\partial x} = 0, \quad \frac{\partial v}{\partial x} = 0, \quad P = 0, \quad \frac{\partial \sigma}{\partial x} = 0.$$

The numerical method used in this study employs the backwards-Euler time-stepping method to identify the evolution of the flow when driven by an AC electric field. The computational domain is discretized into 1001× 701 non-equally spaced grid points in the X- and Y-directions. The calculated solutions are carefully proven to be independent of both the computational grid points and the time step. The detailed description of the iteration algorithm of the numerical method was reported in Luo [23] and Yang and Luo [24].

3. Results and Discussion

3.1 Effect of microchannel width on critical electric field intensity

Fig. 2 illustrates schematic diagram of single T-type microchannel. As shown in the diagram, main channel is 1500μm long, and the wing in Y direction is 700μm long. External DC voltage is applied to the channel inlet, and the mixing channel outlet is grounded. Low-conductivity and high-conductivity solutions are injected into upper and lower inlets respectively at the same time with conductivity ratio of 10:1. In T-type microchannel, two fluids are driven from their respective inlets to the junction of the channel and then flow downstream when external electric field intensity is smaller. Width of the liquid interface gradually expands along the downstream direction as a result of diffusive mixing. The stratified concentration distribution is formed. The stratified fluid continues to flow along the downstream direction when the critical electric field is not attained. In this study, critical electric field intensity is 287V/cm in the 100μm wide channels. As shown in Fig. 3(a), unstable fluctuation occurs on fluid interface, and continues to enlarge along the downstream channel when the external electric field intensity increases to 386V/cm. Figure 3(c) illustrates instantaneous diagram for distribution of conductivity and concentration of fluid flows when constant DC electric field intensity is at bias voltage of 386V/cm. The blue area represents low-conductivity fluid while the red area represents high-conductivity fluid. Greater fluctuation occurred on the interface between two fluids. The fluctuating flow in transverse and longitudinal directions results in a rapid mixing of two streams. This phenomenon is called EKI (electrokinetic instability). These perturbations

gradually grow in shape and size, and occupy the full width of the channel, resulting in chaotic state.

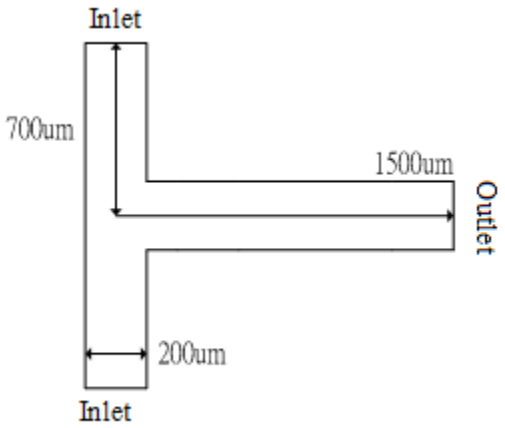

Fig. 2. Schematic diagram of single T-type microchannel.

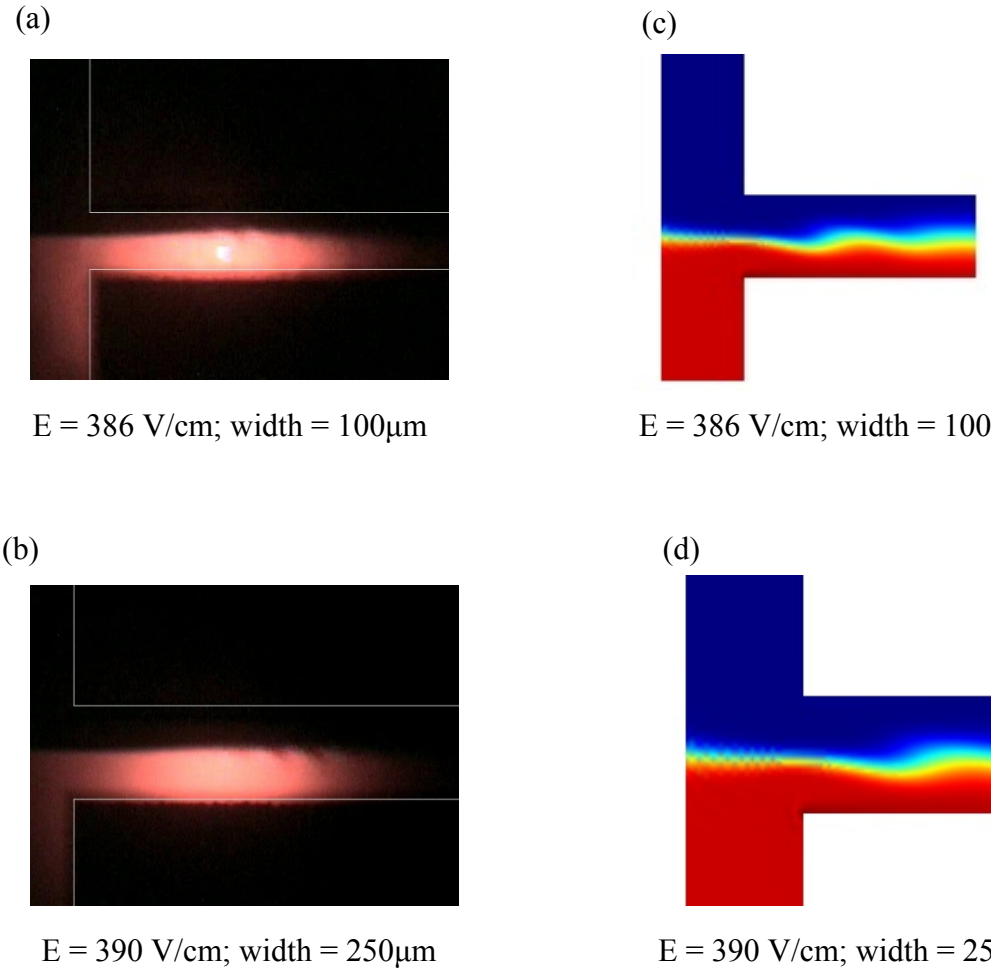

Fig. 3. Fluctuating fluids in single T-type microchannel with width of 100 and 250μm in experiment and simulation.

Table 1 shows comparison of critical electric field intensities in T-type channels with

different widths. From the experiment results, the critical electric field intensity is 287V/cm for 100μm channels, 309 V/cm for 150μm channels, 318V/cm for 200μm channels, and 368V/cm for 250μm channels. The electric conductivity gradient had greater fluctuation on the cross section of 100μm channel. Thus, the critical electric field intensity for the 100μm channel is smaller as compared to the channels of other widths. Namely, narrow channel only needs smaller electric field intensity to achieve EKI. The numerical simulation can also achieve the same result.

Table 1. Critical electric field intensity for single T-type channels with different widths

Critical electric field intensity of T-type channel		
Channel width	Experiment (V/cm)	Simulation (V/cm)
100 μm	287 V/cm	300 V/cm
150 μm	309 V/cm	305 V/cm
200 μm	318 V/cm	310 V/cm
250 μm	368 V/cm	355 V/cm

3.2 Effect of suddenly expanded and reduced T-type microchannel on critical electric field intensity.

In this study, we changed geometric shape of T-type channel (200μm channel), as shown in Fig. 4, including single convex, single concave and biconcave channel structures. The total length and width of the single-convex channel in Fig. 4(a) are the same as the T-type channel in the Figure 2. The difference is at junction of channel below 100μm, the channel is reduced inside by 100μm, with length of 100μm. In Fig. 4(b), at interaction of the channel below 100μm and 300μm, the biconcave channel is reduced inside by 100μm, with length of 100μm. In Fig. 4(c) at junction of channel below 100μm the single convex channel is expanded outside by 100μm with length of 100μm.

Table 2 shows comparison of critical electric field intensity of T-type, single-convex, single-concave and biconcave channels. The critical electric field intensity is 318 V/cm for T-type channel, 409 V/cm for T-type convex channel, 300 V/cm for T-type concave channel and 237 V/cm for T-type biconcave channel. For single concave channel, there is one section with smaller width. The fluid is affected by the channel wall, so two liquids are extruded by wall surface. Electric conductivity gradient between the fluids is greater in narrower cross section of the channel. Thus, EKI may occur on the fluid interface in this area. There are two concave walls with smaller width in the biconcave channel, which extrude the two fluids. EKI may more easily occur on the interface. Besides, perturbation advances towards the outlet. The liquid mixing perturbation is most apparent, and the critical electric field intensity is the smallest. In single convex T-shape channel there is one section with greater width. Thus, electric conductivity gradient in contact with the liquids is smaller, which increases critical electric field intensity required for unstable perturbation. The liquid mixing perturbation is not apparent.

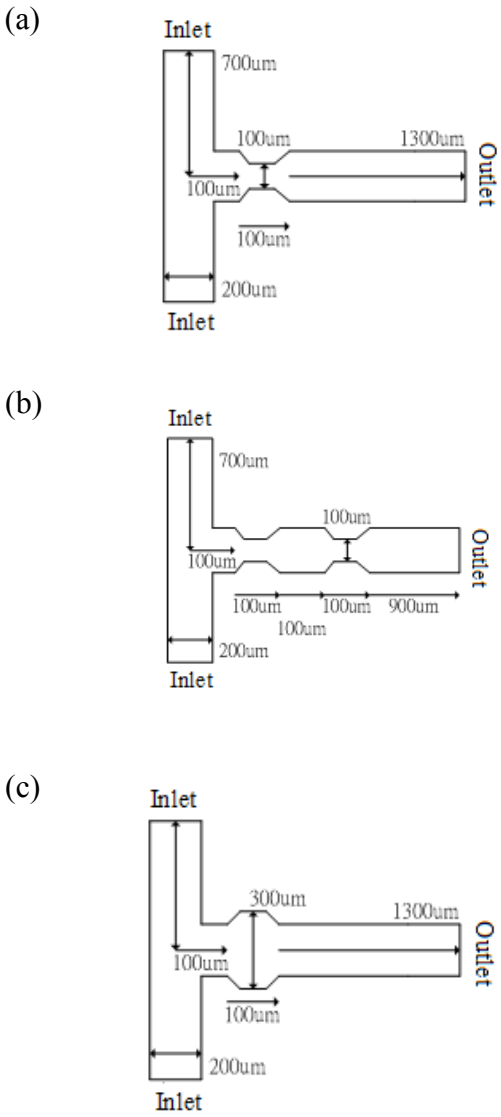

Fig. 4. Schematic diagram of (a) T-type single concave, (b) biconcave and (c) single convex channels

Table 2. Critical electric field intensity for single T-type channels with different geometric shapes.

Critical electric field intensity of T-type channel		
Channel shap	Experiment (V/cm)	Simulation (V/cm)
Single T-type	318 V/cm	310 V/cm
Single convex	409 V/cm	395 V/cm
Single concave	300 V/cm	305 V/cm
Biconcave	237 V/cm	246 V/cm

Figure 5 shows experiments and simulation results of fluid flow instabilities in different geometric shapes. For single convex T-type channel, EKI may occur when the external electric field intensity exceeds critical value of 409V/cm, as shown in Fig. 5(c). Unstable perturbation easily occurs on the fluid interface, especially narrower section of the channel and expands in downstream direction when the external electric field intensity is 454V/cm. Figure 5(f) illustrates

instantaneous concentration distribution of fluid conductivity when constant DC electric field intensity is simulated at bias voltage of 454V/cm. The blue area represents low-conductivity fluid while the red area represents high-conductivity fluid. Greater fluctuation occurred on the fluid interface. The fluctuating flow in transverse and longitudinal directions results in a rapid mixing of two streams. It can be seen that EKI may easily occur in narrower section of channel by observing distribution of conductivity and concentration of fluid flows in simulation.

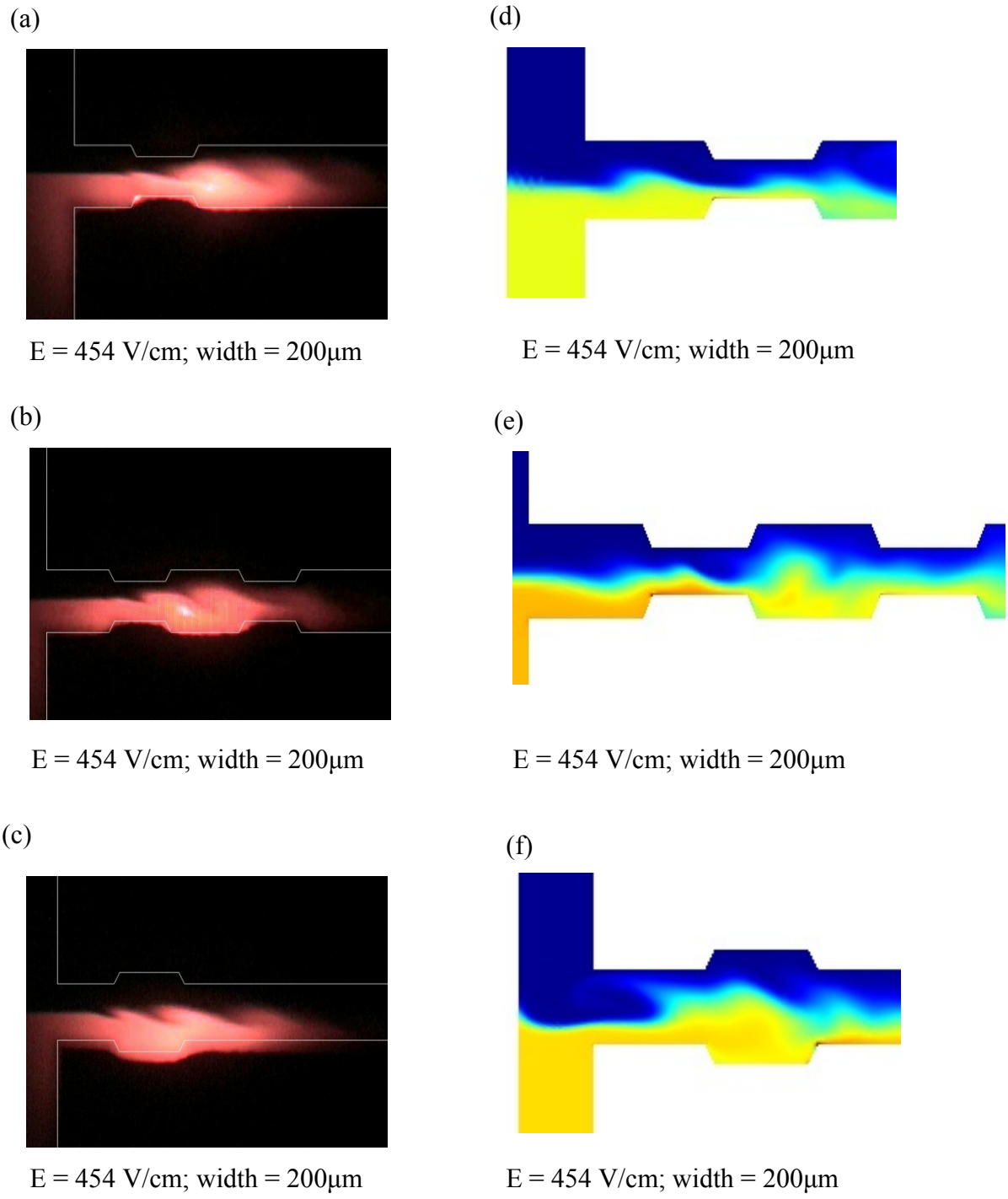

Fig. 5. (a)-(b) Experiment results of fluctuating fluids in single convex, single concave and biconcave channel. (d)-(f) Simulation results of fluctuating fluids

3.3 Effect of suddenly expanded and reduced Cross-shaped microchannel on critical electric field intensity

In this part, we present effect of cross-type microchannel on the critical electric field intensity. Fig. 6 shows structure diagram of cross-type microchannel. In Fig. 6(a), the width of the microchannel is 200μm, length of the left three inlets is 700μm, and the length from junction region of the channel to the outlet is 1500μm. In Fig. 6(b), the channel is reduced inside by 100μm with length of 100μm at junction region of the microchannel below 100μm. In Fig. 6(b), the channel is reduced inside by 100μm with length of 100μm at junction region of the channel below 100μm and 300μm. In Fig. 6(d), the channel is expanded outside by 100μm with length of 100μm at junction region of the channel below 100μm.

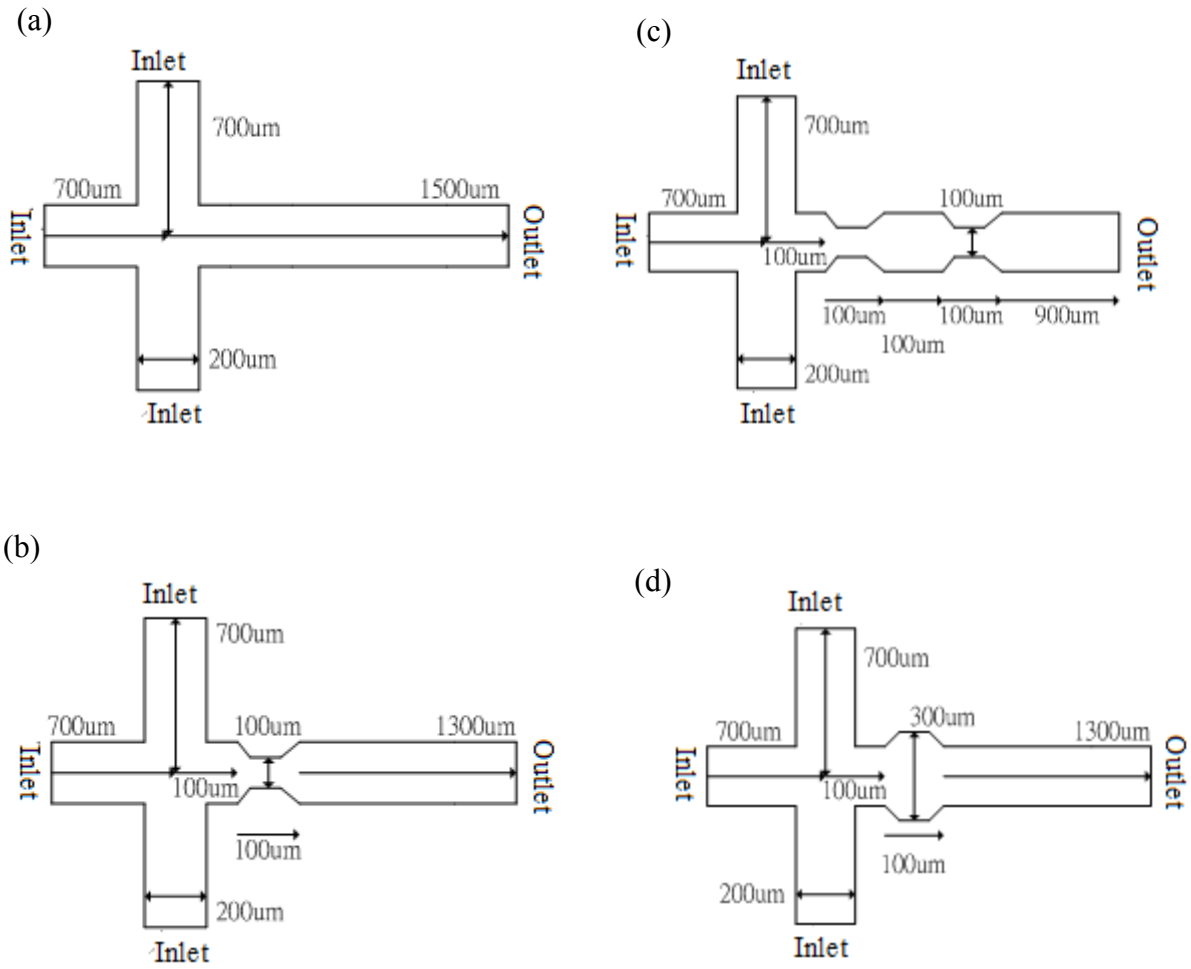

Fig. 6. (a) Schematic diagram of cross-type (b) single concave, (c) biconcave and (d) single convex channels.

3.3.1 Inlet solution with conductivity ratio of 1:10:1

Table 3 shows comparison of critical electric field intensity of cross-type, single-convex, single-concave and biconcave channels. External DC voltage is applied to channel inlet, and the mixing channel outlet is grounded. Low-conductivity solution is injected into upper and lower inlets respectively, and high-conductivity solution is injected into the left inlet, with conductivity ratio of 1:10:1. The critical electric field intensity is 241 V/cm for cross-type channel, 336 V/cm

for single cross-type convex channel, 218 V/cm for the single cross-type concave channel, and 204 V/cm for cross-type biconcave channel. For single concave channel, there is one section with smaller width. The fluid is affected by the channel wall, so two liquids are extruded by wall surface. Electric conductivity gradient between the fluids is greater in narrower cross section of the channel. Thus, EKI may easily occur on the fluid interface in this area. There are two concave walls with smaller width in the biconcave channel, which extrude the two fluids. EKI may more easily occur on the interface. The mixing perturbation of two liquids is most apparent, and the critical electric field intensity is the smallest. There is a section with greater width in the cross-type single convex channel. Because the channel becomes wide and the electric conductivity gradient in contact with the liquid is smaller, the critical electric field intensity increases. The perturbation in mixing of the two liquids is not apparent.

Table .3 Critical electric field intensity for cross-type channels with different geometric shapes (solution conductivity ratio of 1:10:1).

Critical electric field intensity of crtoss-type channel		
Channel shap	Experiment (V/cm)	Simulation (V/cm)
Single cross-type	241 V/cm	253 V/cm
Cross-type convex	336 V/cm	323 V/cm
Cross-type concave	218 V/cm	223 V/cm
Cross-type biconcave	204 V/cm	210 V/cm

The fluids are driven from their respective inlets to the junction of the channel and then flow downstream when external electric field intensity is smaller. Width of the liquid interface gradually expands along the downstream direction as a result of diffusive mixing. The stratified concentration distribution is formed. The stratified liquid continues when the critical electric field is not attained. The fluid flow occurs with unstable perturbation on interface between two liquids if the applied electric field intensity is above the critical value. Figure 7 shows experiments and simulation results of fluid flow instabilities in different geometric shapes. For single convex cross-type channel, EKI occurs when external electric field intensity is above 336V/cm. Figure 7(a) illustrates fluid flow in the channel when the external electric field intensity is 454V/cm. Figure 7(d) shows instantaneous diagram for distribution of fluid conductivity and concentration when constant DC electric field intensity is at bias voltage of 454V/cm. The blue area represents low-conductivity fluid while the red area represents high-conductivity fluid. Greater fluctuation occurs on the interface between two fluids. Based on the results of Figs. 7(a)-(b), no matter what geometric shape is, unstable perturbation may easily occur on narrower fluid interface, and the fluctuating flow in transverse and longitudinal directions results in a rapid mixing of two streams. These perturbations gradually grow downstream. From simulation of fluid conductivity and concentration in the Figs. 7(d)-(f), EKI may easily occur in the narrow section.

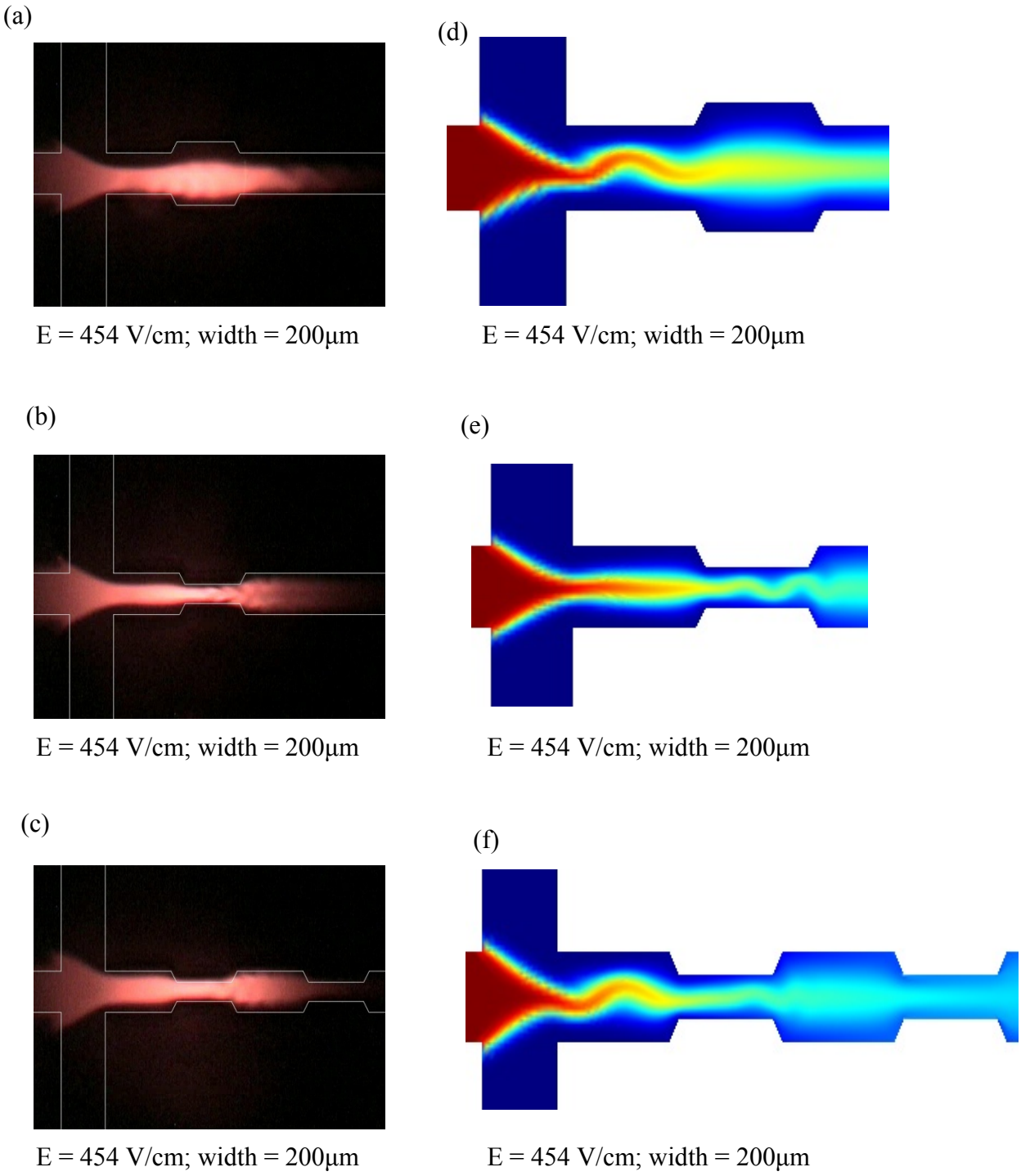

Fig. 7. (a)-(b) Experiment results of fluctuating fluids in single convex, single concave and biconcave channels. (d)-(f) Simulation results of fluctuating fluids.

3.3.2 Inlet solution with conductivity ratio of 10:1:10

Table 4 shows comparison of critical electric field intensity of crossed type, single-convex, single-concave and biconcave channels. For cross-type microchannel, external DC voltage is applied to the inlet channel, and the mixing channel outlet is grounded. In cross-type microchannel, two electrolyte solutions, one with high conductivity and one with low conductivity are introduced

into the microfluidic channels through upper and lower inlets, and left inlet respectively. The conductivity ratio of two fluids is 10:1:10. The critical electric field intensity is 295 V/cm for single cross-type channel, 331 V/cm for single cross-type convex channel, 281 V/cm for single cross-type concave channel, and 254 V/cm for cross-type biconcave channel. For single concave channel, there is one section with smaller width. The fluid is affected by the channel wall, so two liquids are extruded by wall surface. Electric conductivity gradient between the fluids is greater in narrower cross section of the channel. Thus, EKI may easily occur on the fluid interface in this area. There are two concave walls with smaller width in the biconcave channel, which extrude the two fluids. EKI may occur more easily on the interface. The perturbation in mixing of two liquids is most apparent, and the critical electric field intensity is the smallest. There is a section with greater width in the single convex cross-type channel. Because the channel becomes wide and the electric conductivity gradient in contact with the liquid is smaller, the critical electric field intensity increases. The perturbation in mixing of the two liquids is not apparent.

Table 4. Critical electric field intensity for cross-type channels with different geometric shapes (solution conductivity ratio of 10:1:10).

Critical electric field intensity of crtoss-type channel		
Channel shap	Experiment (V/cm)	Simulation (V/cm)
Single cross-type	295 V/cm	300 V/cm
Cross-type convex	331 V/cm	341 V/cm
Cross-type concave	281 V/cm	284 V/cm
Cross-type biconcave	254 V/cm	260 V/cm

The fluids are driven from their respective inlets to the junction region of the channel, and then flow downstream when external electric field intensity is smaller. Width of the liquid interface gradually expands along the downstream direction as a result of diffusive mixing. The stratified concentration distribution is formed. The stratified fluid flow continues when the critical electric field is not attained. The fluctuating flow occurs on the interface between two liquids if the applied electric field intensity is above the critical value. Figure 8 shows experiments and simulation results of fluid flow instabilities in different geometric shapes. As shown in Fig. 8(a), unstable perturbation easily occurs on the fluid interface, especially at narrower section of the channel and expands downstream when the external electric field intensity of single cross-type convex channel is increased to 409V/cm. Figure 8(d) illustrates instantaneous distribution of conductivity and concentration of two fluid flows with different electric conductivity when constant DC electric field intensity is at bias voltage of 409V/cm. The blue area represents low-conductivity fluid and red area represents high-conductivity fluid. In Figs. 8(a)-(c), it can be observed that low-conductivity fluid flow is pearl-like flow. As time elapsed, a string of pearl-like structure flows downstream. Greater fluctuation occurs on the interface between two fluids, and occupies full width of channel. The fluctuating flow in transverse and longitudinal directions results in a rapid mixing of two streams. These perturbations gradually expand in shape and size in downstream direction, and occupy the full width of the channel, resulting in chaotic state. From simulation for distribution of conductivity and concentration of fluid flows in the Figs. 8(d)-(f), EKI easily occurs at the narrower section of the channels.

(a)

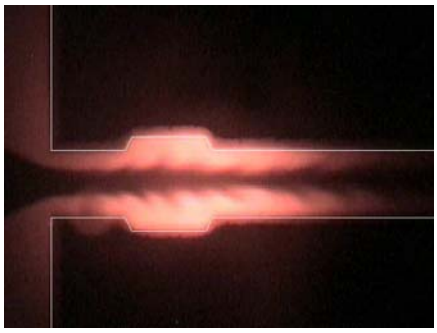

E = 409 V/cm; width = 200μm

(d)

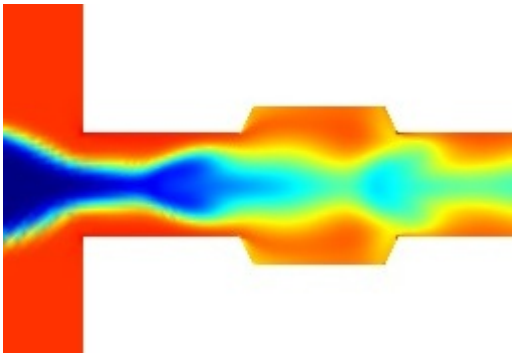

E = 409 V/cm; width = 200μm

(b)

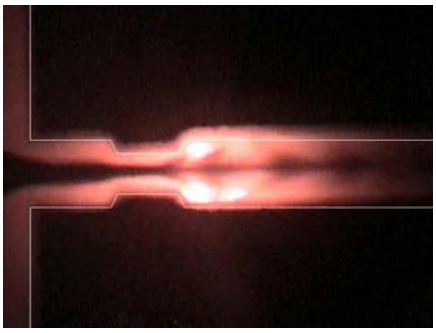

E = 409 V/cm; width = 900μm

(d)

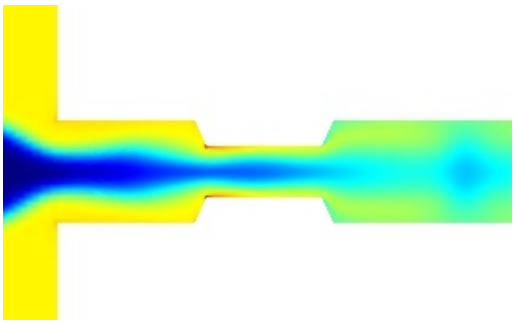

E = 409 V/cm; width = 900μm

(c)

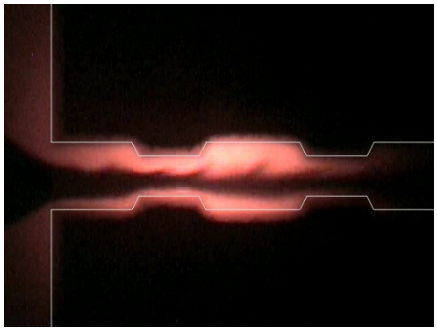

E = 409 V/cm; width = 900μm

(f)

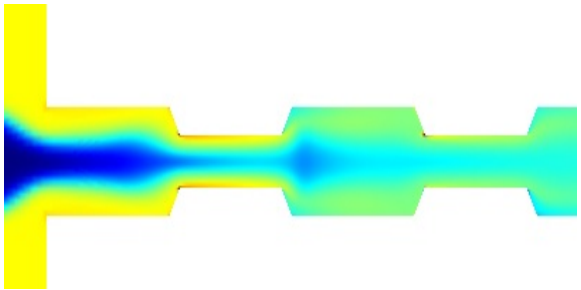

E = 409 V/cm; width = 900μm

Fig. 8 (a)-(b) Experiment results of fluctuating fluids in single convex, single concave and biconcave channels. (d)-(f) Simulation results of fluctuating fluids.

4. Conclusion

In this study, simulation was made for critical electric field intensities of single T-type channels with different widths. The experiment and simulation revealed fluids are affected by channel wall surface when the channel width is smaller. The two liquids are extruded by the wall surface. At narrower cross section of the channels, the electric conductivity gradient between the fluids is greater. Thus, EKI may easily occur on the fluid interface. The critical electric field intensity is smallest. The critical electric field intensities for single T-type microchannels with different widths were summarized. The single T-type channel was compared with T-type sharply expanded and T-type sharply reduced channels in the same width. It has been found that the original critical voltage may vary due to geometric shape of channels. The critical electric field intensity decreases for the sharply reduced channels, and increases for sharply expanded channels. For critical electric field intensity of the 200μm channels, the case of the biconcave T-type is the lowest among the cases investigated.

The cross-type channels and the T-type channels have different channel inlets, but junctions of the channels have the same geometric shape in downstream direction. The liquids are affected by the channel wall surface when they enter into the expanded channel. The channel becomes wide, and the electric conductivity gradient in contact with the liquids is smaller. Thus, the critical electric field intensity increases. The perturbation in mixing of the two liquids is not apparent. When the liquids enter into one section with smaller width in the reduced channel, due to effect of the channel wall, the two liquids are extruded by the wall surface. At narrower cross section of the channel, the electric conductivity gradient between fluids is greater. Thus, EKI occur more easily on the liquid interface. This demonstrates that the critical electric field intensity increase for sharply expanded channel, and decreases for sharply reduced channel. This phenomenon occurs both in the T-type and the cross-type channels.

Acknowledgement

The current authors gratefully acknowledge the financial support provided to this study by the National Science Council of Taiwan under Grant No. NSC 101-2221-E-167-010 and NSC 101-2622-E-167-019-CC3.

References

[1] P.Gravesen, O.J. Branebjerg, S. Jensen, Journal of Micromech. Microeng. **3** 168 (1993)
[2] S. Shoji, Microprocesses and Nanotechnology **99** 72 (1999)
[3] D.J. Harrison, A. Berg, Kluwer Academic Publishers Netherlands (1998)
[4] J. R. Melcher, G.I. Taylor, Annu. Rev. Fluid Mech. **1** 111 (1969)
[5] D. A. Saville, Annu. Rev. Fluid Mech. **29** 27 (1997)
[6] J.F. Hoburg, J.R. Melcher, Phys. Fluids **20** 903 (1977)
[7] J.C. Baygents, F. Baldessari, Phys. Fluids **10** 301 (1998)
[8] H. Lin, B.D. Storey, M.H. Oddy, C. H. Chen, J. G. Santiago, Phys. Fluids **16** 1922 (2004)
[9] M.H. Oddy, J.C. Mikkelsen, J. G. Santiago, Analyt. Chem. **73** 5822 (2001)
[10] J.D. Posner, J.G. Santiago, ASME international Mechanical Engineering congress and Exposition November 13-20 (2004)
[11] C.H. Chen, H. Lin, S.K. Lele, J.G. Santiago, Journal of Fluid Mechanics **524** 263 (2005)
[12] S.M. Shin, I.S. Kang, Y.K. Cho, Journal of Micromech. Microeng. **15** 455, (2005)
[13] J. Park, S. M. Shin, K.Y. Huh, I.S. Kang, Physics of Fluids **17** 118101 (2005)
[14] M.H. Oddy, C.H. Chen, J. G. Santiago, Physics of Fluid **16**, 1922 (2004)
[15] C.H. Tai, R.J. Yang, L.M. Fu, Electrophoresis **27** 4982 (2006)
[16] Y.J. Pan, C.M. Ren, R.J. Yang, Journal of Micromech. Microeng. **17** 820 (2007)

[17] W.J. Luo, K.F. Yarn, M.H. Shih, C. K. Yu, Optoelectron. Adv. Mater. – Rapid Commun. **2** 117 (2008)
[18] J.S. Chen, K.F. Yarn, S.F. Cheng, W.J. Luo, M.H. Chung, Dig J Nanomater Bios. **6**(2) 391 (2011)
[19] K.F. Yarn, Y.J. Pan, W.J. Luo, C.N. Chen, Dig J Nanomater Bios. 7(4) 1735 (2012)
[20] J.K. Chen, W.J. Luo, R.J. Yang, Japanese Journal of Applied Physics **45**(10A) 7983 (2006)
[21] C.C. Cho, C.L. Chen, C.K. Chen, Chemical Engineering Journal **191** 132 (2012)
[22] C.H. Lin, G.B. Lee, Y.H. Lin, G.L. Chang, Journal of Micromech. Microeng. **11** 726 (2001)
[23] W.J. Luo, Journal of Colloid and Interface Science **295**(2) 551 (2006)
[24] R.J. Yang, W. J. Luo, Theory Comput. Fluid Dyn. **16** 115 (2002)